

# Exclusive $J/\psi$ and $\Upsilon$ hadroproduction and the QCD odderon

A. Bzdak<sup>a</sup>, L. Motyka<sup>a,b</sup>, L. Szymanowski<sup>c,d,e</sup> and J.-R. Cudell<sup>c</sup>

<sup>a</sup> *M. Smoluchowski Institute of Physics, Jagellonian University, Kraków, Poland*

<sup>b</sup> *II Institute of Theoretical Physics, Hamburg University, Hamburg, Germany*

<sup>c</sup> *Université de Liège, B4000 Liège, Belgium*

<sup>d</sup> *CPHT, École Polytechnique, CNRS, 91128 Palaiseau, France*

<sup>e</sup> *Soltan Institute for Nuclear Studies, Warsaw, Poland*

## Abstract

We study  $pp$  and  $p\bar{p}$  collisions which lead to the exclusive production of  $J/\psi$  or  $\Upsilon$  from the pomeron–odderon and the pomeron–photon fusion. We calculate scattering amplitudes of these processes in the lowest order approximation and in the framework of  $k_\perp$ –factorization. We present estimates of cross sections for the kinematic conditions of the Tevatron and of the LHC.

## 1 Introduction

It follows from the optical theorem that total cross sections of hadronic processes are driven by colour singlet exchanges in the  $t$ –channel. Thus, pomeron exchange, characterized by an even charge parity, gives the dominant contribution to the sum of the direct and the crossed amplitudes for a given hadronic process. The exchange with the odd charge parity, i.e. that of the odderon, dominates the difference between these two amplitudes. The concept of the odderon in the description of hadronic processes was introduced a long time ago [1]. Although it is a partner of the pomeron, which is well known from the study of diffractive processes, the odderon still remains a mystery. As it differs from the

pomeron only by its charge parity, one would expect, from the point of view of general principles based on the analyticity and the unitarity of the  $S$ -matrix, that its exchange should lead to effects of a comparable magnitude to those coming from pomeron exchange. However, the odderon still escapes experimental verification.

In perturbative QCD, the pomeron is modeled by two interacting gluons in a colour-singlet state, whereas the odderon is described by an analogous system formed by three gluons. It is thus quite natural to expect that in hard processes the effects of odderon exchange — being suppressed by an additional power of the strong coupling constant  $\alpha_s$  — are smaller than similar contributions due to pomeron exchange. This was confirmed by QCD studies of the diffractive exclusive  $\eta_c$  production mediated by odderon exchange [2–5], which led to rather small cross sections. It was surprising, however, that a non-perturbative description within the stochastic vacuum model of the similar exclusive process of the  $\pi^0$  production [6] gave a prediction which was disproved by experiment [7]. It was then argued that the suppression of the  $\pi_0$  photoproduction may emerge as a result of the chiral symmetry constraints on the photon- $\pi_0$  coupling [8] or of the odderon absorption by its coupling to the pomeron [9].

A natural difficulty in detecting odderon effects in inclusive measurements is the fact that, in general, the odderon exchange yields only a small correction to the dominating pomeron contribution to the scattering amplitude. On the other hand, this difficulty can be overcome in some cases by studying the charge asymmetries caused by simultaneous pomeron and odderon exchanges [10]. This measurement looks rather promising but it was not performed yet, and to this day the best, but still weak, experimental evidence for the odderon was found as a difference between the differential elastic cross sections for  $pp$  and  $p\bar{p}$  scattering in the diffractive dip region at  $\sqrt{s} = 53$  GeV at the CERN ISR [11]. For a detailed review of the phenomenological and theoretical status of the odderon we refer the reader to Ref. [12].

In the present paper, we study the exclusive production of an heavy vector meson,  $V = J/\psi, \Upsilon$ , in  $pp$  and  $p\bar{p}$  collisions:  $pp(\bar{p}) \rightarrow p' V p''(\bar{p}'')$ ; for a recent review of meson hadroproduction see e.g. [13]. We consider the production of the meson in the central rapidity region, separated (in rapidity) from the two outgoing hadrons  $p'$  and  $p''(\bar{p}'')$  by two rapidity gaps. The vector meson results thus from pomeron-odderon fusion. The mass of the heavy vector meson supplies the hard scale in the process of fusion, which may justify a description of the pomeron and the odderon within perturbative QCD. The above contribution competes naturally with the production of the meson in pomeron-photon fusion, which is, however, under much better theoretical control.

Diffractive production of the  $J/\psi$  meson in proton-(anti)proton collisions via pomeron-odderon fusion was investigated already in Ref. [14] in the framework of Regge theory. The potential contribution of the  $\omega$  reggeon to this process is expected to be strongly suppressed due to the Zweig rule. The estimate of the total  $J/\psi$  production cross section

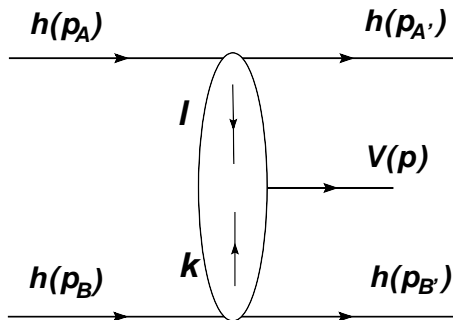


Figure 1: *Kinematics of the exclusive meson production in  $pp$  ( $p\bar{p}$ ) scattering.*

to be of the order of 75 nb is quite encouraging<sup>1</sup>.

In this paper we estimate using perturbative QCD the pomeron–odderon and pomeron–photon contributions to the exclusive  $J/\psi$  and  $\Upsilon$  hadroproduction, assuming the Tevatron and the LHC conditions. We find that the exclusive heavy vector meson production in  $pp$  and  $p\bar{p}$  collisions may serve as a useful tool in odderon searches. The resulting cross sections for pomeron–odderon fusion are large enough to yield large production rates already at the Tevatron for the  $J/\psi$  and for the  $\Upsilon$  at the LHC. The “background” photon-driven sub-process is estimated to have a similar cross section to the pomeron–odderon contribution, and in order to clearly isolate the odderon one should perform a careful analysis of the transverse momentum distributions of the outgoing particles.

The structure of the paper is the following. Section 2 contains a summary of the kinematics. In Section 3 we derive the scattering amplitudes for the two mechanisms of meson hadroproduction. Since the calculational technique which we use is rather well-known, we present mostly final results, whereas technical details are given in the Appendix. Section 4 presents our predictions as well as their discussion.

## 2 Kinematics

We study the processes of hadroproduction shown in Fig. 1,

$$h(p_A) + h(p_B) \rightarrow h(p_{A'}) + V(p) + h(p_{B'}), \quad (1)$$

where  $h$  and  $V$  denote an (anti)proton and a  $J/\psi$  (or  $\Upsilon$ ) meson, respectively. In the high-energy limit we neglect the mass of the (anti)proton  $h$  and we identify the momenta  $p_A$  and  $p_B$  with two light-like Sudakov vectors,  $p_A^2 = p_B^2 = 0$ , so that the scattering energy squared equals  $s = (p_A + p_B)^2 = 2p_A \cdot p_B$ .

The momenta of the outgoing particles are parametrized as

---

<sup>1</sup>This result does not take the pomeron–photon fusion contribution into account.

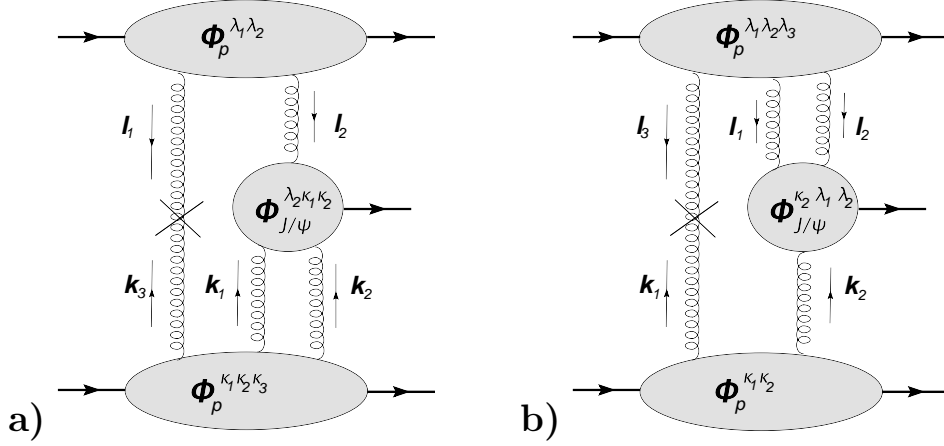


Figure 2: The lowest order diagrams defining the pomeron-odderon fusion amplitudes for vector meson production a)  $\mathcal{M}_{PO}$  and b)  $\mathcal{M}_{OP}$ .

$$p_{A'} = (1 - x_A)p_A + \frac{l^2}{s(1 - x_A)}p_B - l_\perp \quad \text{with} \quad l^2 = -l_\perp \cdot l_\perp, \quad (2)$$

$$p_{B'} = \frac{k^2}{s(1 - x_B)}p_A + (1 - x_B)p_B - k_\perp$$

and

$$p = \alpha_p p_A + \beta_p p_B + p_\perp$$

$$\alpha_p = x_A - \frac{k^2}{s(1 - x_B)} \approx x_A, \quad \beta_p = x_B - \frac{l^2}{s(1 - x_A)} \approx x_B, \quad p_\perp = l_\perp + k_\perp, \quad (3)$$

which lead to the mass-shell condition for the vector meson,  $V = J/\psi, \Upsilon$ ,

$$m_V^2 = s x_A x_B - (l + k)^2. \quad (4)$$

### 3 The impact-factor representation of scattering amplitudes

It is well known that at high energies and for small momentum transfers a natural framework to calculate the scattering amplitude of the process (1) is the  $k_\perp$ -factorization method, see e.g. [15], [2–4] and references therein. According to this approach, the amplitude is represented as convolutions, over two-dimensional transverse momenta of  $t$ -channel partonic reggeons, of the impact factors describing scattered nucleons and of the effective production vertex of the vector meson. The leading power of  $s$  contributing to the scattering amplitude comes from  $t$ -channel exchanges of gluonic reggeons.

In the lowest-order approximation, the contributions to the production of  $J/\psi$  from pomeron-odderon fusion are shown in Figs. 2a, b. The pomeron and the odderon are

described in this approximation as non-interacting longitudinally polarized exchanges of two and three gluons, respectively. The two gluons from the odderon which couple to the effective production vertex of the  $J/\psi$  will involve the symmetric constants  $d^{abc}$  of the colour algebra. The competing production process of  $J/\psi$  from pomeron–photon fusion is illustrated in Figs. 3a, b.

Let us first consider proton–proton scattering. The impact factor representation of the diagrams shown in Fig. 2a reads (see Appendix A1 for details)

$$\begin{aligned} \mathcal{M}_{PO} = & \quad (5) \\ & -is \frac{2 \cdot 3}{2! 3!} \frac{4}{(2\pi)^8} \int \frac{d^2 \mathbf{l}_1}{\mathbf{l}_1^2} \frac{d^2 \mathbf{l}_2}{\mathbf{l}_2^2} \delta^2(\mathbf{l}_1 + \mathbf{l}_2 - \mathbf{l}) \frac{d^2 \mathbf{k}_1}{\mathbf{k}_1^2} \frac{d^2 \mathbf{k}_2}{\mathbf{k}_2^2} \frac{d^2 \mathbf{k}_3}{\mathbf{k}_3^2} \delta^2(\mathbf{k}_1 + \mathbf{k}_2 + \mathbf{k}_3 - \mathbf{k}) \\ & \times \delta^2(\mathbf{k}_3 + \mathbf{l}_1) \mathbf{k}_3^2 \delta^{\lambda_1 \kappa_3} \cdot \Phi_P^{\lambda_1 \lambda_2}(\mathbf{l}_1, \mathbf{l}_2) \cdot \Phi_P^{\kappa_1 \kappa_2 \kappa_3}(\mathbf{k}_1, \mathbf{k}_2, \mathbf{k}_3) \cdot \Phi_{J/\psi}^{\lambda_2 \kappa_1 \kappa_2}(\mathbf{l}_2, \mathbf{k}_1, \mathbf{k}_2) . \end{aligned}$$

Here  $\Phi_P^{\lambda_1 \lambda_2}(\mathbf{l}_1, \mathbf{l}_2)$  denotes the impact factor of the proton, scattered via pomeron exchange. The gluons forming the pomeron with the momenta  $\mathbf{l}_1, \mathbf{l}_2$  carry the colour indices  $\lambda_1, \lambda_2$ , respectively. The corresponding impact factor of the proton, scattered via odderon exchange, is denoted as  $\Phi_P^{\kappa_1 \kappa_2 \kappa_3}(\mathbf{k}_1, \mathbf{k}_2, \mathbf{k}_3)$ . Again,  $\kappa_1, \kappa_2, \kappa_3$  are the colour indices of gluons with the momenta  $\mathbf{k}_1, \mathbf{k}_2, \mathbf{k}_3$ . The effective production vertex of the  $J/\psi$  meson is denoted  $\Phi_{J/\psi}^{\lambda_2 \kappa_1 \kappa_2}(\mathbf{l}_2, \mathbf{k}_1, \mathbf{k}_2)$ . It results from the fusion of a gluon with the momentum and the colour index  $(\mathbf{l}_2, \lambda_2)$  from the pomeron with two gluons  $(\mathbf{k}_1, \kappa_1)$  and  $(\mathbf{k}_2, \kappa_2)$  of the odderon. In order to keep the notation of momenta  $\mathbf{l}_i$  and  $\mathbf{k}_j$  most symmetric, we introduced an additional, artificial vertex (denoted by the cross in Fig. 2)  $\delta^2(\mathbf{k}_3 + \mathbf{l}_1) \mathbf{k}_3^2 \delta^{\lambda_1 \kappa_3}$  connecting the spectator gluons  $(\mathbf{l}_1, \lambda_1)$  and  $(\mathbf{k}_3, \kappa_3)$ . The ratio  $\frac{2 \cdot 3}{2! 3!} = \frac{1}{2}$  is a combinatorial factor. The factors  $\frac{1}{2!}$  and  $\frac{1}{3!}$  correct the over-counting of diagrams introduced by factorization in the scattering amplitudes of the impact factor with pomeron and odderon exchanges, respectively. The factor  $2 \cdot 3 = 6$  accounts for all possibilities to build the spectator gluon from the momenta  $\mathbf{l}_i$  and  $\mathbf{k}_j$ .

The proton impact factors  $\Phi_P^{\lambda_1 \lambda_2}(\mathbf{l}_1, \mathbf{l}_2)$  and  $\Phi_P^{\kappa_1 \kappa_2 \kappa_3}(\mathbf{k}_1, \mathbf{k}_2, \mathbf{k}_3)$  are “soft”, non-perturbative objects, therefore to determine their form we need some non-perturbative model of nucleon structure. In our estimates we use the phenomenological eikonal model of impact factors proposed by Fukugita and Kwieciński [16] (the FK model). The impact factors can be determined in two steps. Firstly, the impact factors of a single quark are calculated in the way described in Refs. [2–4, 15]. Although these calculations are now quite standard, nevertheless in order to make our paper self-contained and to fix the normalization of the impact factors and of the production vertices, we present some technical details in the Appendix. The quark impact factor corresponding to the pomeron exchange as in Fig. 2a reads (see Appendix A2 for details)

$$\Phi_q^{\lambda_1 \lambda_2}(\mathbf{l}_1, \mathbf{l}_2) = -\bar{g}^2 \cdot 2\pi \cdot \frac{\delta^{\lambda_1 \lambda_2}}{2 N_c} = -\bar{\alpha}_s \cdot 8\pi^2 \cdot \frac{\delta^{\lambda_1 \lambda_2}}{2 N_c} , \quad (6)$$

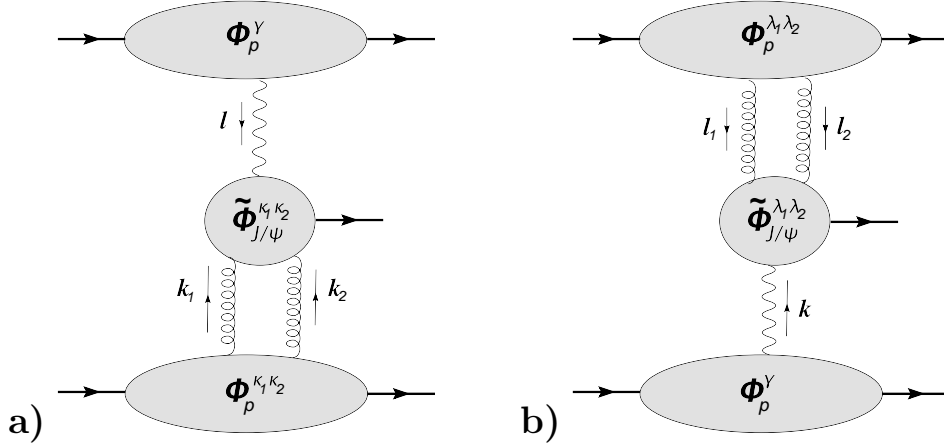


Figure 3: The lowest order diagrams defining the pomeron-photon fusion amplitudes of the vector meson production a)  $\mathcal{M}_{\gamma P}$  and b)  $\mathcal{M}_{P\gamma}$ .

whereas the corresponding expression with the odderon exchange has the form

$$\Phi_q^{\kappa_1 \kappa_2 \kappa_3}(\mathbf{k}_1, \mathbf{k}_2, \mathbf{k}_3) = i \bar{g}^3 (2\pi)^2 \frac{d^{\kappa_3 \kappa_2 \kappa_1}}{4N_c} = i \bar{\alpha}_s^{\frac{3}{2}} 2^5 \pi^{\frac{7}{2}} \frac{d^{\kappa_3 \kappa_2 \kappa_1}}{4N_c}, \quad (7)$$

with  $\bar{\alpha}_s$  — the effective coupling constant in the soft region,  $\bar{\alpha}_s = \bar{g}^2/(4\pi)$  and  $d^{\kappa_3 \kappa_2 \kappa_1}$  the symmetric structure constants of the colour  $SU(3)$  group. The value of the effective coupling constant  $\bar{\alpha}_s$  in Eqs. (6,7) is one of the main sources of theoretical uncertainties in our estimates and we shall return to this problem in the final discussion.

Secondly, the internal structure of the nucleon is taken into account by “dressing” the quark impact factors with phenomenological form factors. These form factors should be chosen in a way consistent with the gauge invariance of QCD, i.e. they should vanish when either of momenta  $\mathbf{l}_i$  or  $\mathbf{k}_j$  vanishes. In the case of pomeron exchange, the proton impact factor is modeled as

$$\Phi_P^{\lambda_1 \lambda_2}(\mathbf{l}_1, \mathbf{l}_2) = 3 \mathcal{F}_P(\mathbf{l}_1, \mathbf{l}_2) \Phi_q^{\lambda_1 \lambda_2}(\mathbf{l}_1, \mathbf{l}_2), \quad (8)$$

with

$$\mathcal{F}_P(\mathbf{l}_1, \mathbf{l}_2) = F(\mathbf{l}_1 + \mathbf{l}_2, 0, 0) - F(\mathbf{l}_1, \mathbf{l}_2, 0), \quad (9)$$

where the function  $F(\mathbf{k}_1, \mathbf{k}_2, \mathbf{k}_3)$  is taken in the form

$$F(\mathbf{k}_1, \mathbf{k}_2, \mathbf{k}_3) = \frac{A^2}{A^2 + \frac{1}{2}((\mathbf{k}_1 - \mathbf{k}_2)^2 + (\mathbf{k}_2 - \mathbf{k}_3)^2 + (\mathbf{k}_3 - \mathbf{k}_1)^2)}, \quad (10)$$

with  $A$  being a phenomenological constant chosen to be half of the  $\rho$  meson mass,  $A = m_\rho/2 \approx 384$  MeV. The structure of expression (9) is quite natural: the first term on the r.h.s. of (9) corresponds to the contribution in which two gluons couple to the same quark line, the second term represents two gluons coupling to two different quarks, whereas the factor 3 in (8) counts the number of valence quarks inside the proton.

The corresponding expression for the proton impact factor with the odderon exchange is constructed in a similar way, as

$$\Phi_P^{\kappa_1 \kappa_2 \kappa_3}(\mathbf{k}_1, \mathbf{k}_2, \mathbf{k}_3) = 3 \mathcal{F}_O(\mathbf{k}_1, \mathbf{k}_2, \mathbf{k}_3) \Phi_q^{\kappa_1 \kappa_2 \kappa_3}(\mathbf{k}_1, \mathbf{k}_2, \mathbf{k}_3), \quad (11)$$

where the form-factor  $\mathcal{F}_O$  has the form

$$\mathcal{F}_O(\mathbf{k}_1, \mathbf{k}_2, \mathbf{k}_3) = F(\mathbf{k} = \mathbf{k}_1 + \mathbf{k}_2 + \mathbf{k}_3, 0, 0) - \sum_{i=1}^3 F(\mathbf{k}_i, \mathbf{k} - \mathbf{k}_i, 0) + 2 F(\mathbf{k}_1, \mathbf{k}_2, \mathbf{k}_3), \quad (12)$$

where the function  $F$  is defined by Eq. (10). Again, the first term on the r.h.s. of Eq. (12) corresponds to a contribution when all three gluons couple to a single valence quark, the three terms  $F(\mathbf{k}_i, \mathbf{k} - \mathbf{k}_i, 0)$  describe the cases when a gluon with momentum  $\mathbf{k}_i$  and two gluons with total momentum  $\mathbf{k} - \mathbf{k}_i$  couple to two different quarks and the last term describes a coupling of the three gluons to the three different valence quarks of a nucleon.

Let us also note that anti-proton impact factors, i.e.  $\Phi_{\bar{P}}^{\kappa_1 \kappa_2}$  for pomeron exchange and  $\Phi_{\bar{P}}^{\kappa_1 \kappa_2 \kappa_3}$  for odderon exchange, are easily obtained from the proton ones: they are given by the same expressions, the only modification is the additional minus sign for the impact factor of odderon exchange, related to its opposite charge parity

$$\Phi_{\bar{P}}^{\kappa_1 \kappa_2} = \Phi_P^{\kappa_1 \kappa_2}, \quad \Phi_{\bar{P}}^{\kappa_1 \kappa_2 \kappa_3} = -\Phi_P^{\kappa_1 \kappa_2 \kappa_3}. \quad (13)$$

The derivation of the effective production vertex of a charmonium  $\Phi_{J/\psi}^{\lambda_2 \kappa_1 \kappa_2}(\mathbf{l}_2, \mathbf{k}_1, \mathbf{k}_2)$  as a part of the impact factor representation (5) is one of the main results of the present study. For that we assume that the mass  $m_{J/\psi}$  of charmonium supplies a sufficiently hard scale so we can rely on perturbation theory. The charmonium is treated in the non-relativistic approximation, where the  $\bar{c}c \rightarrow J/\psi$  production vertex has the form

$$\langle \bar{c} c | J/\psi \rangle = \frac{g_{J/\psi}}{2} \hat{\varepsilon}^*(p) (p \cdot \gamma + m_{J/\psi}), \quad m_{J/\psi} = 2m_c, \quad (14)$$

where we assume that the  $\bar{c} c$  pair is in the colour singlet state,  $\varepsilon^*$  is the polarization vector of the charmonium. The coupling constant  $g_{J/\psi}$  in (14) is expressed in terms of the electronic width  $\Gamma_{e^+e^-}^{J/\psi}$  of the  $J/\psi \rightarrow e^+e^-$  decay

$$g_{J/\psi} = \sqrt{\frac{3m_{J/\psi}\Gamma_{e^+e^-}^{J/\psi}}{16\pi\alpha_{em}^2 Q_c^2}}, \quad Q_c = \frac{2}{3}. \quad (15)$$

The effective production vertex  $\Phi_{J/\psi}^{\lambda_2 \kappa_1 \kappa_2}$  as drawn in Fig. 2a can be viewed as being closely related to the usual impact factor describing the transition of a virtual photon  $\gamma^*$  into  $J/\psi$  via pomeron exchange. Indeed, it is a crossed version of the latter, with the  $s$ -channel  $\gamma^*$  replaced by the  $t$ -channel gluon of virtuality  $-\mathbf{l}_2^2$  and with two gluons  $\mathbf{k}_2$  and  $\mathbf{k}_3$  in the symmetric  $8_S$  colour representation, instead of the (also symmetric) colour-singlet one.

Consequently, the calculation of the  $\Phi_{J/\psi}^{\lambda_2 \kappa_1 \kappa_2}$  vertex can proceed in a way analogous to that of the impact factor of the transition  $\gamma^* \rightarrow J/\psi$  [15]. We thus obtain as a result (technical details of derivation are presented in Appendix A3)

$$\begin{aligned} \Phi_{J/\psi}^{\lambda_2 \kappa_1 \kappa_2}(\mathbf{l}_2, \mathbf{k}_1, \mathbf{k}_2) &= g^3 \frac{d^{\kappa_1 \kappa_2 \lambda_2}}{N_c} V_{J/\psi}(\mathbf{l}_2, \mathbf{k}_1, \mathbf{k}_2) = \alpha_s^{\frac{3}{2}} 8\pi^{\frac{3}{2}} \frac{d^{\kappa_1 \kappa_2 \lambda_2}}{N_c} V_{J/\psi}(\mathbf{l}_2, \mathbf{k}_1, \mathbf{k}_2), \\ V_{J/\psi}(\mathbf{l}_2, \mathbf{k}_1, \mathbf{k}_2) &= \\ 4\pi m_c g_{J/\psi} &\left[ -\frac{x_B \varepsilon^* \cdot p_B + \varepsilon^* \cdot l_{2\perp}}{l_2^2 + (\mathbf{k}_1 + \mathbf{k}_2)^2 + 4m_c^2} + \frac{\varepsilon^* \cdot l_{2\perp} + \varepsilon^* \cdot p_B \left( x_B - \frac{4\mathbf{k}_1 \cdot \mathbf{k}_2}{sx_A} \right)}{l_2^2 + (\mathbf{k}_1 - \mathbf{k}_2)^2 + 4m_c^2} \right]. \end{aligned} \quad (16)$$

Let us note that, with the mass-shell condition (4) taken into account, the expression (16) vanishes when either of the momenta  $\mathbf{l}_2$ ,  $\mathbf{k}_2$  or  $\mathbf{k}_3$  vanishes. This property is a consequence of the QCD gauge invariance, that guarantees the infra-red convergence of the integrals in the impact-factor representation (5).

The impact-factor representation of the diagrams shown in Fig. 2b,  $\mathcal{M}_{OP}$ , is obtained from the previous formulae by the following replacement of the momenta and of the colour indices

$$\mathcal{M}_{OP} = \mathcal{M}_{PO} |_{(\mathbf{l}_i, \lambda_i) \rightarrow (\mathbf{k}_i, \kappa_i), (\mathbf{k}_j, \kappa_j) \rightarrow (\mathbf{l}_j, \lambda_j), x_A \leftrightarrow x_B}. \quad (17)$$

Passing to a description of  $J/\psi$  production in pomeron–photon fusion, the impact-factor representation of the diagrams shown in Fig. 3a reads (see Appendix A1)

$$\begin{aligned} \mathcal{M}_{\gamma P} &= \\ -\frac{1}{2!} \cdot s \cdot \frac{4}{(2\pi)^4 l^2} \Phi_P^\gamma(\mathbf{l}) &\int \frac{d^2 \mathbf{k}_1}{\mathbf{k}_1^2} \frac{d^2 \mathbf{k}_2}{\mathbf{k}_2^2} \delta^2(\mathbf{k}_1 + \mathbf{k}_2 - \mathbf{k}) \Phi_P^{\kappa_1 \kappa_2}(\mathbf{k}_1, \mathbf{k}_2) \tilde{\Phi}_{J/\psi}^{\kappa_1 \kappa_2}(\mathbf{l}, \mathbf{k}_1, \mathbf{k}_2). \end{aligned} \quad (18)$$

Here again, the factor  $\frac{1}{2!}$  accounts for the over-counting of diagrams introduced by the factorization of the scattering amplitude involving the proton impact factor with the pomeron exchange, Eq. (8).

The photon coupling to the proton involves a phenomenological form factor, which we take as

$$\Phi_P^\gamma(\mathbf{l}) = -ie \cdot F(\mathbf{l}, 0, 0). \quad (19)$$

It has a proper normalization, with the  $-ie$  coupling, when  $\mathbf{l} \rightarrow 0$ . When the proton is replaced by an anti-proton, it changes sign

$$\Phi_P^\gamma(\mathbf{l}) = -\Phi_{\bar{P}}^\gamma(\mathbf{l}), \quad (20)$$

similarly to the case of the odderon exchange, Eq. (13).

The effective production vertex of charmonium in pomeron–photon fusion is, modulo a different colour factor and coupling constants, identical to the one in pomeron–odderon fusion (16), see Appendix A3 for details. We obtain

$$\tilde{\Phi}_{J/\psi}^{\kappa_1 \kappa_2}(\mathbf{l}, \mathbf{k}_1, \mathbf{k}_2) = g^2 e Q_c \frac{2\delta^{\kappa_1 \kappa_2}}{N_c} V_{J/\psi}(\mathbf{l}, \mathbf{k}_1, \mathbf{k}_2) = \alpha_s e Q_c 8\pi \frac{\delta^{\kappa_1 \kappa_2}}{N_c} V_{J/\psi}(\mathbf{l}, \mathbf{k}_1, \mathbf{k}_2), \quad (21)$$



with  $V_{J/\psi}(\mathbf{l}, \mathbf{k}_1, \mathbf{k}_2)$  given by Eq. (16).

Also, let us note that the impact-factor representation of the scattering amplitude corresponding to the diagrams shown in Fig. 3b,  $\mathcal{M}_{P\gamma}$ , is obtained from (18) by the following substitution of momenta and colour indices

$$\mathcal{M}_{P\gamma} = \mathcal{M}_{\gamma P} |_{(\mathbf{k}_i, \kappa_i) \rightarrow (\mathbf{l}_j, \lambda_j), x_A \leftrightarrow x_B} , \quad (22)$$

analogously to the substitution (17) in the case of pomeron–odderon fusion.

The comparison of the impact-factor representations (5) and (18) for the two mechanisms of hadroproduction, together with the formulas for the impact factors and the effective vertices, leads to the conclusion that, due to different numbers of factors  $i$  in both amplitudes, they differ by a relative complex phase factor  $e^{i\pi/2}$ . It means that the odderon and the photon contributions to the cross section do not interfere.

Finally, let us mention that, by replacing  $m_{J/\psi}$ ,  $g_{J/\psi}$  and  $Q_c$  characterizing the charmonium  $J/\psi$  by  $m_\Upsilon$ ,  $g_\Upsilon$  and  $Q_b = 1/3$ , the formulae of this section describe the exclusive hadroproduction of the bottomium  $\Upsilon$ .

## 4 Estimates for the cross section and discussion

An evaluation of the odderon contribution to the exclusive production cross sections of the heavy vector mesons in  $pp$  and  $p\bar{p}$  collisions was performed numerically. The starting point of this evaluation is the amplitude for pomeron–odderon fusion

$$\mathcal{M}_{PO}^{\text{tot}} = \mathcal{M}_{PO} + \mathcal{M}_{OP}, \quad (23)$$

calculated separately for each of the independent polarisation vectors  $\varepsilon$  of the outgoing vector meson. We focused on an unpolarised cross section, so that the cross sections were summed over all the polarisations. We consider therefore,

$$\frac{d\sigma}{dy} = \sum_{\varepsilon} \int_{t_{\min}^A}^{t_{\max}^A} dt_A \int_{t_{\min}^B}^{t_{\max}^B} dt_B \int_0^{2\pi} d\phi \frac{d\sigma^{(\varepsilon)}}{dy dt_A dt_B d\phi} , \quad (24)$$

where

$$\frac{d\sigma^{(\varepsilon)}}{dy dt_A dt_B d\phi} = \frac{1}{512\pi^4 s^2} |\mathcal{M}_{PO}^{\text{tot}}|^2, \quad (25)$$

is a differential cross section for the meson polarisation  $\varepsilon$ ,  $t_A = \mathbf{l}^2$ ,  $t_B = \mathbf{k}^2$ ,  $\phi$  is the azimuthal angle between  $\mathbf{k}$  and  $\mathbf{l}$  and  $y \simeq \frac{1}{2} \log(x_A/x_B)$  is the rapidity of the meson in the colliding hadrons c.m. frame. The lower limits  $t_{\min}^A$  and  $t_{\min}^B$  are set to zero for pomeron–odderon fusion. The pomeron–photon fusion cross section,  $d\sigma_\gamma/dy$ , may be obtained from Eqs. (23,24,25) by the replacements  $\mathcal{M}_{PO} \rightarrow \mathcal{M}_{P\gamma}$ ,  $\mathcal{M}_{OP} \rightarrow \mathcal{M}_{\gamma P}$  etc. The resulting  $\frac{d\sigma_\gamma}{dy dt_A dt_B}$ , however, exhibits the usual singular behaviour  $\sim 1/t_i$ ,  $i = A, B$  at  $t_i \rightarrow 0$ , due to the photon propagator. A standard kinematic analysis, used e.g. in the

Weizsäcker–Williams approximation, provides a lower kinematic cut-off on the photon virtuality, giving  $t_{\min}^A \simeq m_p^2 x_A^2$  and  $t_{\min}^B \simeq m_p^2 x_B^2$ , with  $m_p$  denoting the proton mass (see, e.g. [17]). The upper limit  $t_{\max}$  could be, in principle, arbitrarily large, but the model of the proton impact factor is unreliable at larger  $t$ , thus we set  $t_{\max} = 1.44 \text{ GeV}^2$ .

In the model applied no QCD evolution has been taken into account so far and the resulting unpolarised pomeron–odderon differential cross section (25) does not depend explicitly on the total collision energy and on the rapidity of the produced vector meson. In order to get reliable predictions for the cross sections this should be corrected. In what follows, we shall take into account the effects of BFKL evolution [18] and the effects of soft-rescattering which tend to destroy the rapidity gap.

We shall include the effects of the BFKL evolution of the pomeron using a phenomenological enhancement factor  $E(s, m_V)$ , with  $V = J/\psi, \Upsilon$ . Note also that the model parameter  $\bar{\alpha}_s$  enters the pomeron–odderon fusion cross section in the fifth power, which may lead to significant uncertainty of the results. Thus, for clarity of the discussion, the parameter  $\bar{\alpha}_s$  will be explicitly isolated in the presentation of the numerical results. In addition, the obtained formulae should be corrected for multiple soft re-scatterings of proton which can destroy the rapidity gap [19]. Those effects will be expressed as a gap survival factor  $S_{\text{gap}}^2$ . Thus, a more realistic cross section, that takes into account necessary phenomenological improvements may be written as

$$\left. \frac{d\sigma^{\text{corr}}}{dy} \right|_{y=0} = \bar{\alpha}_s^5 S_{\text{gap}}^2 E(s, m_V) \frac{d\sigma}{dy}, \quad (26)$$

where  $d\sigma/dy$  is the cross section given by (24) at  $\bar{\alpha}_s = 1$ .

The calculation is valid only in the high energy limit, which implicitly constrains the allowed energy and rapidity range, say for  $x_A < x_0$  and  $x_B < x_0$ , and we set  $x_0 = 0.1$ . In numerical evaluations we focus on the central  $J/\psi$  and  $\Upsilon$  production,  $y \simeq 0$ , where  $x_A \simeq x_B \simeq m_V/\sqrt{s}$ . We approximate the effects of QCD evolution of the pomeron amplitude by an exponential enhancement factor  $\exp(\lambda \Delta y)$  where  $\Delta y \simeq \log(x_0/x_A)$  is the rapidity evolution length of the QCD pomeron. Thus, for the central production one obtains

$$E(s, m_V) = (x_0 \sqrt{s}/m_V)^{2\lambda}. \quad (27)$$

The effective pomeron intercept  $\lambda$  depends on the hard scale involved in the process (see, e.g. [20]). Following HERA results on the the pomeron intercept in exclusive vector meson production we take  $\lambda = 0.2$  ( $\lambda = 0.35$ ) for the  $J/\psi$  ( $\Upsilon$ ) production [21, 22]. Thus,  $E(s, m_V)$  gives a substantial enhancement by a factor of about 5 and 12 (about 9 and 33) for the  $J/\psi$  ( $\Upsilon$ ) production at the Tevatron and the LHC correspondingly. For the odderon, the rapidity evolution given by the Bartels–Kwieciński–Praszałowicz equation [23] leads to a flat dependence on the gap size<sup>2</sup>, so we neglect the rapidity dependence of the odderon.

---

<sup>2</sup>This is true for the Bartels–Lipatov–Vacca solution [24] at large rapidities and approximately true for the Janik–Wosiek solution [25].

Note, that we shall not change the meson production vertex in the pomeron–odderon fusion by including into it an (unknown yet) analogue of the Sudakov suppression factor for the case of three outgoing gluons. An inclusion of the Sudakov-like form-factor would be a desirable improvement but the consistent way of taking its effects into account requires simultaneously a more detailed analysis of the effects of QCD evolution of proton impact factors which is beyond the scope of this paper.

The strong coupling constant in the meson impact factor was set to  $\alpha_s(m_c) = 0.38$  ( $\alpha_s(m_b) = 0.21$ ), in accordance with the QCD running. Recall that we assume that  $m_c = m_{J/\psi}/2$  and analogously in the case of  $\Upsilon$ ,  $m_b = m_\Upsilon/2$ . The available estimates of the effective strong coupling constant,  $\bar{\alpha}_s$ , of the Fukugita–Kwieciński model, yield results with rather large spread. The constraints from the data on the total  $pp$  and  $p\bar{p}$  cross sections gave  $\bar{\alpha}_s = 0.7 - 0.9$  [16] and a recent thorough analysis of the odderon exchange contribution to the elastic  $pp$  and  $p\bar{p}$  scattering [26] bounds the coupling to be much smaller,  $\bar{\alpha}_s \simeq 0.3$ . Thus, we performed an independent test of the model based on the vector meson photoproduction data. Using the FK model we found the following amplitude of  $J/\psi$  photoproduction off proton in the forward direction:

$$\mathcal{M}_\gamma = is \pi e Q_c \bar{\alpha}_s \alpha_s(m_c) g_{J/\psi} \frac{N_c^2 - 1}{N_c^2} \frac{3 \log(3m_c^2/A^2)}{m_c(m_c^2 - A^2/3)}, \quad (28)$$

and the  $t$ -dependence (determined numerically) was found to agree reasonably well with the experimentally measured  $\exp(-Bt)$ , for moderate  $t$ , with  $B \simeq 4.5 \text{ GeV}^{-2}$ . Thus, we compared the model estimate of the  $J/\psi$  exclusive photoproduction cross-section to the data at  $W \simeq 10 \text{ GeV}$ , (equivalent to pomeron  $x \simeq x_0$ ) and we obtained  $\bar{\alpha}_s \simeq 0.6 - 0.7$ .

The estimate of uncertainties introduced by  $\bar{\alpha}_s$  and  $S_{\text{gap}}^2$  should be carried out together. The reason for that is that the low value of  $\bar{\alpha}_s \simeq 0.3$  was obtained from an estimate of the odderon exchange in which the soft gap survival factor was neglected, thus when it was set  $S_{\text{gap}}^2 = 1$ . Therefore, for consistency, we shall also use  $S_{\text{gap}}^2 = 1$  in our calculation if the low value of  $\bar{\alpha}_s = 0.3$  is taken. This combination  $S_{\text{gap}}^2 = 1$  and  $\bar{\alpha}_s = 0.3$  gives low cross-sections and it will be called the *pessimistic scenario*.

In the *optimistic scenario* we shall use a large value of the coupling,  $\bar{\alpha}_s = 1$ , combined with the gap survival factors obtained in the Durham two-channel eikonal model:  $S_{\text{gap}}^2 = 0.05$  for the exclusive production at the Tevatron and  $S_{\text{gap}}^2 = 0.03$  for the LHC [19, 27], see also [28]. We believe that the best estimates should follow from the *central scenario* defined by  $\bar{\alpha}_s = 0.75$ ,  $S_{\text{gap}}^2 = 0.05$  ( $S_{\text{gap}}^2 = 0.03$ ) at the Tevatron (LHC).

We analyze the pomeron–photon contribution in a way analogous to the pomeron–odderon contribution. In the case of photon exchange, the  $pp$  ( $p\bar{p}$ ) scatter typically at large impact parameters and we assume that the gap survival  $S_{\text{gap}}^2 \simeq 1$  in this case.<sup>3</sup>

---

<sup>3</sup>A more detailed analysis of the gap survival for the photon exchange was performed in Ref. [29]. In the same reference a crude estimate of the pomeron–odderon fusion was obtained, based on the assumption that the whole odderon is coupled to the single quark (anti-quark) line.

$d\sigma/dy$	$J/\psi$		$\Upsilon$	
	odderon	photon	odderon	photon
$p\bar{p}$	20 nb	1.6 nb	36 pb	1.1 pb
$pp$	11 nb	2.3 nb	21 pb	1.7 pb

Table 1: *Naïve cross sections  $d\sigma/dy$  given by (24) for the exclusive  $J/\psi$  and  $\Upsilon$  production in  $pp$  and  $p\bar{p}$  collisions by the odderon-pomeron fusion, assuming  $\bar{\alpha}_s = 1$  and analogous cross sections  $d\sigma_\gamma/dy$  for the photon contribution. The numbers given are partial results only and they must be improved phenomenologically to provide reliable predictions.*

Thus, we arrive at the analogue of Eq. 26 for the photon:

$$\left. \frac{d\sigma_\gamma^{\text{corr}}}{dy} \right|_{y=0} = \bar{\alpha}_s^2 E(s, m_V) \frac{d\sigma_\gamma}{dy}. \quad (29)$$

Numerical results for  $d\sigma/dy$  and  $d\sigma_\gamma/dy$  are listed in Table 1. The photon cross sections depend on the total collision energy  $\sqrt{s}$  through the kinematic dependence of the lower cut-offs  $t_{\text{min}}^A$  and  $t_{\text{min}}^B$ . Thus, the photon cross sections in Table 1 for the  $p\bar{p}$  and the  $pp$  case were obtained assuming the kinematics of the central production at the Tevatron ( $\sqrt{s} = 2$  TeV) and at the LHC ( $\sqrt{s} = 14$  TeV) respectively. Note that there is a significant difference between the  $pp$  and  $p\bar{p}$  cross sections indicating a significant interference between the pomeron–odderon and the odderon–pomeron contributions. We stress that the numbers in Table 1 represent only partial results, and they are displayed to provide a basis for estimates of realistic cross-sections and their uncertainties, according to the prescription given above.

Besides the cross sections integrated over transverse momenta, we calculated also the differential distributions of the produced vector mesons, defined as

$$\left. \frac{d\sigma}{dy d\mathbf{p}^2} \right|_{\text{norm}} = \left( \frac{d\sigma}{dy} \right)^{-1} \times \sum_{\varepsilon} \int_{\mathbf{k}^2 < t_{\text{max}}} d^2k \int_{\mathbf{l}^2 < t_{\text{max}}} d^2l \frac{d\sigma^{(\varepsilon)}}{dy d^2k d^2l} \delta((\mathbf{k} + \mathbf{l})^2 - \mathbf{p}^2). \quad (30)$$

In Fig. 4a and 4b we show the normalised distributions for the  $J/\psi$  (and the  $\Upsilon$ ) production in  $p\bar{p}$  and  $pp$  collisions respectively. Clearly, the shapes only weakly depend on the vector meson flavour.<sup>4</sup> The production of vector mesons in the forward direction ( $\mathbf{p}^2 = 0$ ) is maximal for  $p\bar{p}$  collisions and vanishes for  $pp$  collisions. This striking difference is caused by an already mentioned interference between the pomeron–odderon and the odderon–pomeron contributions.

The magnitudes of the phenomenologically improved cross sections are summarized in Table 2. They were calculated using formulae (26) and (29) accounting for the QCD

---

<sup>4</sup>An apparent discrepancy in the normalisation of the  $J/\psi$  and  $\Upsilon$  distributions visible in Fig. 4b emerges because we show only part of the  $\mathbf{p}^2$ -distributions.

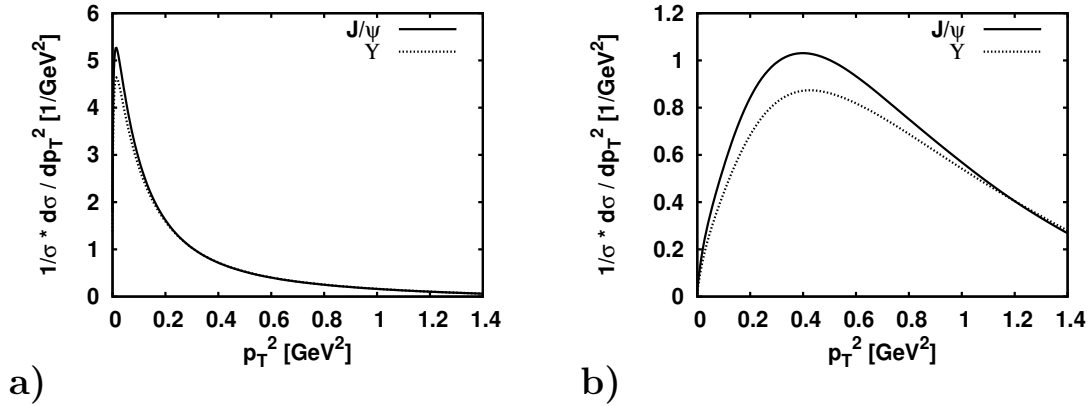


Figure 4:  $\frac{d\sigma}{dy d\mathbf{p}^2} \Big|_{\text{norm}}$  for a)  $p\bar{p} \rightarrow p\bar{p}V$  and b)  $pp \rightarrow ppV$ .

evolution of the pomeron and the gap survival factor, and the uncertainty of  $\bar{\alpha}_s$  was taken into account, according to the three scenarios that we consider. Recall that the photon and the odderon contributions do not interfere in the lowest order approximation and the corresponding cross sections may be treated independently. As seen from the table, the pomeron–odderon contributions are found to be uncertain, with a multiplicative uncertainty factor of 3–5. The ambiguities, however, cancel partially in the ratio of the pomeron–odderon contribution to the pomeron–photon contribution evaluated in the same scenario. Thus, within the considered scenarios, the “odderon to photon ratio”  $R = [d\sigma^{\text{corr}}/dy]/[d\sigma_{\gamma}^{\text{corr}}/dy]$  varies between 0.3 and 0.6 for  $J/\psi$  production at the Tevatron, and between about 0.06 and 0.15 at the LHC. In the case of  $\Upsilon$ ,  $R$  varies between about 0.8 and 1.7 at the Tevatron and between about 0.15 and 0.4 at the LHC. These numbers suggest that the odderon contribution may well be of a similar magnitude to the photon contribution at the Tevatron and somewhat smaller than the photon contribution at the LHC.

Let us note here that the photon-mediated vector meson hadroproduction may be calculated in a different manner using the Weizsäcker–Williams approximation. The dominance of very low virtualities in the photon propagator permits to treat one of the protons as a source (with a suitable form factor) of quasi-real photons that collide with the other proton and produce the vector mesons [29, 30]. In this approximation, the quasi-real photon flux is convoluted with a cross-section of the meson photoproduction off the proton. The  $J/\psi$  photoproduction was measured rather accurately at HERA [21, 22] and one may use parametrisations of HERA data to perform necessary extrapolations. In this approach theoretical uncertainties and model dependencies are greatly reduced. Thus, calculations based on the Weizsäcker–Williams approximation combined with fits to the HERA data give  $d\sigma/dy(p\bar{p} \rightarrow p\bar{p}J/\psi)|_{y=0} \simeq 2 - 2.5$  nb [29, 30], somewhat lower than our central scenario. For the  $\Upsilon$  production at the LHC, predictions of Ref. [30]:  $d\sigma/dy(pp \rightarrow pp\Upsilon)|_{y=0} \simeq 100$  pb are larger than ours by a factor of more than three.

$d\sigma^{\text{corr}}/dy$	$J/\psi$		$\Upsilon$	
	odderon	photon	odderon	photon
Tevatron	0.3–1.3–5 nb	0.8–5–9 nb	0.7–4–15 pb	0.8–5–9 pb
LHC	0.3–0.9–4 nb	2.4–15–27 nb	1.7–5–21 pb	5–31–55 pb

Table 2: Cross sections  $d\sigma^{\text{corr}}/dy|_{y=0}$  given by (26) for the exclusive  $J/\psi$  and  $\Upsilon$  production in  $pp$  and  $p\bar{p}$  collisions by the pomeron–odderon fusion, and analogous cross sections  $d\sigma_{\gamma}^{\text{corr}}/dy|_{y=0}$  for the photon contribution given by (29) for the pessimistic–central–optimistic scenarios.

This suggests that the odderon exchange predictions for the  $\Upsilon$  production may also be underestimated in the central scenario.

Our calculations indicate that the odderon-to-photon ratio tends to be of the order of unity or smaller, which makes it difficult to get a clear signal of the odderon from the integrated cross sections. The ratio, however, may be enhanced if suitable cuts on outgoing protons transverse momenta are imposed. Namely, the photon exchange is dominated by very small photon virtualities (as it follows e.g. from the Weizsäcker–Williams approximation), and, for instance for  $t_A, t_B > 0.25 \text{ GeV}^2$  the pomeron–odderon fusion contribution decreases by about one order of magnitude, being still visible, and the pomeron–photon fusion contribution decreases by more than two orders of magnitude. Then, the odderon contribution could well be a few times larger than the photon contribution. Thus, a careful analysis of the outgoing proton momenta distribution should permit clear identification of the odderon and the photon contributions.

As a final point, let us indicate briefly the possibility to probe the odderon via the  $\Upsilon$  hadroproduction at the LHC in an asymmetric kinematic situation, using the forward detectors, as for instance the planned forward proton spectrometer FP420 [31]. This detector may be capable of measuring the outgoing proton energy and transverse momentum with a very good accuracy, for protons that would lose about 1% of their energy. This corresponds to  $x_A \simeq 0.01$  (see Section 2). For  $\Upsilon$  production in the exclusive process it leads to  $x_B = m_{\Upsilon}^2/(sx_A) \simeq 5 \cdot 10^{-5}$ . The bottomonium emerging at the rapidity  $y_{\Upsilon} \simeq 2.7$  should be possible to detect in the  $\mu^+\mu^-$  decay channel, and the proton  $p_B$  would escape detection. Clearly, due to the small- $x$  evolution of the pomeron, the dominant contribution to the production amplitude should then come from the pomeron propagating across the large rapidity gap, related to  $x_B$ , and the odderon or photon should span the smaller rapidity gap, given by  $x_A$ . More precisely, for  $x_A \gg x_B$ , the amplitudes  $\mathcal{M}_{OP}$  and  $\mathcal{M}_{\gamma P}$  shown in Fig. 2b and Fig. 3a respectively are enhanced by the QCD evolution by a factor of  $(x_A/x_B)^{\lambda} \simeq 6$  with respect to the amplitude  $\mathcal{M}_{PO}$  and  $\mathcal{M}_{P\gamma}$ . Therefore, in this kinematics the proton  $p_A$  couples predominantly to the odderon and to the photon, and one could use the difference in  $l^2$ –dependence of the photon and the odderon exchange to cut on the proton momentum  $p_A$ :  $l^2 > l_{\text{min}}^2$ , and filter out partially the pomeron–photon

contribution. An additional advantage of the measurement in this asymmetric kinematics is that at  $y_T \simeq 2.7$  the pomeron evolution down to  $x_B$  provides an overall enhancement by a factor of a few of the exclusive  $\Upsilon$  hadroproduction cross section with respect to the central production, leading to comfortably large cross sections, well in reach of the LHC.

## Acknowledgments

We acknowledge useful discussions with J. Bartels, C. Ewerz, K. Golec-Biernat, O. Nachtmann, B. Pire and S. Wallon. This work is partly supported by the Polish (MEiN) research grants 1 P03B 028 28, N202 060 31/3199, and by the Fonds National de la Recherche Scientifique (FNRS, Belgium). L.Sz. and L.M. acknowledge a warm hospitality extended to them at Ecole Polytechnique and at LPT-Orsay.

## A Appendix

### A.1 Derivation of the impact-factor representation (5) and (18)

The sum of the Feynman diagrams describing the fusion of the pomeron (two gluons with total momentum  $l$ ) with the odderon (three gluons with total momentum  $k$ ) is written in the Feynman gauge as

$$\begin{aligned} \mathcal{M}_{PO} = & -i \frac{1}{2! 3!} \int \frac{d^4 l_1 d^4 l_2}{(2\pi)^4} \delta^4(l_1 + l_2 - l) \frac{d^4 k_1 d^4 k_2 d^4 k_3}{(2\pi)^8} \delta^4(k_1 + k_2 + k_3 - k) \\ & \mathcal{S}_{\mu_1 \mu_2}^{\lambda_1 \lambda_2}(A \rightarrow A') \frac{(-ig^{\mu_1 \mu'_1})}{l_1^2 + i\epsilon} \frac{(-ig^{\mu_2 \mu'_2})}{l_2^2 + i\epsilon} \mathcal{S}_{\mu'_1 \mu'_2; \nu'_1 \nu'_2 \nu'_3}^{\lambda_1 \lambda_2; \kappa_1 \kappa_2 \kappa_3}(J/\psi) \\ & \frac{(-ig^{\nu_1 \nu'_1})}{k_1^2 + i\epsilon} \frac{(-ig^{\nu_2 \nu'_2})}{k_2^2 + i\epsilon} \frac{(-ig^{\nu_3 \nu'_3})}{k_3^2 + i\epsilon} \mathcal{S}_{\nu_1 \nu_2 \nu_3}^{\kappa_1 \kappa_2 \kappa_3}(B \rightarrow B'). \end{aligned} \quad (\text{A.1})$$

Here  $\mathcal{S}_{\mu_1 \mu_2}^{\lambda_1 \lambda_2}(A \rightarrow A')$  is the  $S$ -matrix element describing the transition of the hadronic state  $A$  into  $A'$  through the exchange of two gluons with momenta  $l_i$ ,  $i = 1, 2$ . The  $S$ -matrix carries Lorentz and colour indices  $\mu_i$  and  $\lambda_i$ , respectively.  $\mathcal{S}_{\nu_1 \nu_2 \nu_3}^{\kappa_1 \kappa_2 \kappa_3}(B \rightarrow B')$  is the  $S$ -matrix element describing the transition of hadronic state  $B$  into  $B'$  through the exchange of three gluons with momenta  $k_j$ ,  $j = 1, 2, 3$ . It carries also Lorentz and colour indices  $\nu_i$  and  $\kappa_i$ , respectively. Finally,  $\mathcal{S}_{\mu'_1 \mu'_2; \nu'_1 \nu'_2 \nu'_3}^{\lambda_1 \lambda_2; \kappa_1 \kappa_2 \kappa_3}(J/\psi)$  is the  $S$ -matrix element describing the fusion of the two gluons forming the pomeron with the three gluons forming the odderon which produces the  $J/\psi$ . The  $S$ -matrices in Eq. (A.1) are connected by the gluonic propagators in the Feynman gauge. The factorization of the scattering amplitude  $\mathcal{M}_{PO}$  in terms of the  $S$ -matrices of different subprocesses is possible by introducing an overcounting of contributing diagrams which gets compensated by the combinatorial factor  $1/(2! 3!)$ .

The gluonic fusion which results in the production of  $J/\psi$  involves only three gluons in the lowest order of perturbation theory. It means, that in  $\mathcal{S}_{\mu'_1\mu'_2;\nu'_1\nu'_2\nu'_3}^{\lambda_1\lambda_2;\kappa_1\kappa_2\kappa_3}(J/\psi)$  one of the two gluons  $l_i$  together with one of three gluons  $k_j$  form the spectator gluon, disconnected from the  $S$ -matrix describing fusion. Such spectator gluon can be formed in  $2 \cdot 3 = 6$  ways and each of these possibilities contributes equally to the scattering amplitude  $\mathcal{M}_{PO}$ . It means that we can consider only one such choice, e.g. with the spectator formed by gluons  $l_1$  and  $k_3$ , and multiply the corresponding result by 6. The formula for  $\mathcal{M}_{PO}$  can be thus put in the form

$$\begin{aligned} \mathcal{M}_{PO} = & -i \frac{6}{2! 3!} \int \frac{d^4 l_1 d^4 l_2}{(2\pi)^4} \delta^4(l_1 + l_2 - l) \frac{d^4 k_1 d^4 k_2 d^4 k_3}{(2\pi)^8} \delta^4(k_1 + k_2 + k_3 - k) \\ & i(2\pi)^4 \delta^4(l_1 + k_3) g_{\mu'_1\nu'_3} k_3^2 \delta^{\lambda_1\kappa_3} \mathcal{S}_{\mu_1\mu_2}^{\lambda_1\lambda_2}(A \rightarrow A') \frac{(-ig^{\mu_1\mu'_1})}{l_1^2 + i\epsilon} \frac{(-ig^{\mu_2\mu'_2})}{l_2^2 + i\epsilon} \mathcal{S}_{\mu'_2;\nu'_1\nu'_2}^{\lambda_2\kappa_1\kappa_2}(J/\psi) \\ & \frac{(-ig^{\nu_1\nu'_1})}{k_1^2 + i\epsilon} \frac{(-ig^{\nu_2\nu'_2})}{k_2^2 + i\epsilon} \frac{(-ig^{\nu_3\nu'_3})}{k_3^2 + i\epsilon} \mathcal{S}_{\nu_1\nu_2\nu_3}^{\kappa_1\kappa_2\kappa_3}(B \rightarrow B'). \end{aligned} \quad (\text{A.2})$$

Here,  $\mathcal{S}_{\mu'_2;\nu'_1\nu'_2}^{\lambda_2\kappa_1\kappa_2}(J/\psi)$  is the  $S$ -matrix element of the fusion of gluons with the momenta  $l_2$ ,  $k_1$  and  $k_2$ . We write also the artificial vertex  $i(2\pi)^4 \delta^4(l_1 + k_3) g_{\mu'_1\nu'_3} k_3^2 \delta^{\lambda_1\kappa_3}$  to ensure the most symmetric notation of the different parts of expression (A.2) in the momenta  $l_i$ ,  $k_j$ .

The formula (A.2) can be further rewritten by applying standard approximations valid in Regge kinematics, i.e. characterising processes occuring at high-energies, with small momentum transfers. The dominant contribution in  $s$  to the scattering amplitude is obtained from the longitudinal polarizations of the  $t$ -channel gluons. It results from the following substitution of numerators in the gluonic propagators

$$g^{\mu_i\mu'_i} \rightarrow \frac{p_B^{\mu_i} p_A^{\mu'_i}}{p_A \cdot p_B}, \quad g^{\nu_j\nu'_j} \rightarrow \frac{p_A^{\nu_j} p_B^{\nu'_j}}{p_A \cdot p_B}, \quad (\text{A.3})$$

and leads to the highest power of large scalar products  $p_A \cdot p_B = s/2$ .

We parametrize all momenta using the Sudakov decompositions

$$l_i = \alpha_{li} p_A - \beta_{li} p_B + l_{\perp i}, \quad k_j = -\alpha_{kj} p_A + \beta_{kj} p_B + k_{\perp j}, \quad (\text{A.4})$$

so that  $d^4 l_i = p_A \cdot p_B d\alpha_{li} d\beta_{li} d^2 l_{\perp i}$  and  $d^4 k_j = p_A \cdot p_B d\alpha_{kj} d\beta_{kj} d^2 k_{\perp j}$ .

In the Regge kinematics, the values of the longitudinal Sudakov parameters of the gluons in the  $t$ -channels are strongly ordered. As a result, in the  $S$ -matrix  $\mathcal{S}_{\mu_1\mu_2}^{\lambda_1\lambda_2}(A \rightarrow A')$ , one can neglect the dependence on the parameters  $\alpha_{li}$ , as they are much smaller than the  $\alpha$  components of other momenta characterizing the transition  $h(p_A) \rightarrow h(p_{A'})$ . Similarly, in the  $S$ -matrix  $\mathcal{S}_{\nu_1\nu_2\nu_3}^{\kappa_1\kappa_2\kappa_3}(B \rightarrow B')$  one can neglect the dependence on  $\beta_{kj}$ . On the other hand, the  $S$ -matrix  $\mathcal{S}_{\mu'_2;\nu'_1\nu'_2}^{\lambda_2\kappa_1\kappa_2}(J/\psi)$  depends effectively only on  $\alpha_{l2} \approx \alpha_p \approx x_A$  and  $\beta_{k1}, \beta_{k2}$ , subject to the condition  $\beta_{k1} + \beta_{k2} \approx \beta_p \approx x_B$ .

In the high energy limit, the asymptotics of the scattering amplitude  $\mathcal{M}_{PO}$  is determined by small values of the longitudinal Sudakov parameters. Consequently, the



denominators of the gluon propagators are given by contributions coming only from the transverse components of the momenta

$$l_i^2 \approx l_{\perp i}^2 = -\mathbf{l}_i^2, \quad k_j^2 \approx k_{\perp j}^2 = -\mathbf{k}_j^2. \quad (\text{A.5})$$

All the above remarks permit to represent  $\mathcal{M}_{PO}$  as a convolution in transverse momenta of  $t$ -channel gluons

$$\begin{aligned} \mathcal{M}_{PO} = & \quad (\text{A.6}) \\ & -is \frac{6}{2!} \frac{4}{3!} \frac{1}{(2\pi)^8} \int \frac{d^2 \mathbf{l}_1}{\mathbf{l}_1^2} \frac{d^2 \mathbf{l}_2}{\mathbf{l}_2^2} \delta^2(\mathbf{l}_1 + \mathbf{l}_2 - \mathbf{l}) \frac{d^2 \mathbf{k}_1}{\mathbf{k}_1^2} \frac{d^2 \mathbf{k}_2}{\mathbf{k}_2^2} \frac{d^2 \mathbf{k}_3}{\mathbf{k}_3^2} \delta^2(\mathbf{k}_1 + \mathbf{k}_2 + \mathbf{k}_3 - \mathbf{k}) \\ & \delta^2(\mathbf{l}_1 + \mathbf{k}_3) \mathbf{k}_3^2 \delta^{\lambda_1 \kappa_3} \int d\beta_{l_1} \mathcal{S}_{\mu_1 \mu_2}^{\lambda_1 \lambda_2}(A \rightarrow A') \frac{p_B^{\mu_1} p_B^{\mu_2}}{s} \int d\alpha_{k_3} d\alpha_{k_1} \mathcal{S}_{\nu_1 \nu_2 \nu_3}^{\kappa_1 \kappa_2 \kappa_3}(B \rightarrow B') \frac{p_A^{\nu_1} p_A^{\nu_2} p_A^{\nu_3}}{s} \\ & \int d\beta_{k_1} \mathcal{S}_{\mu'_2 \nu'_1 \nu'_2}^{\lambda_2 \kappa_1 \kappa_2}(J/\psi) \frac{p_A^{\mu'_2} p_B^{\nu'_1} p_B^{\nu'_2}}{s}, \end{aligned}$$

which coincides with Eq. (5) if one defines the impact-factor for pomeron exchange as

$$\Phi_P^{\lambda_1 \lambda_2}(\mathbf{l}_1, \mathbf{l}_2) = \int d\beta_{l_1} \mathcal{S}_{\mu_1 \mu_2}^{\lambda_1 \lambda_2}(A \rightarrow A') \frac{p_B^{\mu_1} p_B^{\mu_2}}{s}, \quad (\text{A.7})$$

the impact-factor for odderon exchange as

$$\Phi_P^{\kappa_1 \kappa_2 \kappa_3}(\mathbf{k}_1, \mathbf{k}_2, \mathbf{k}_3) = \int d\alpha_{k_3} d\alpha_{k_1} \mathcal{S}_{\nu_1 \nu_2 \nu_3}^{\kappa_1 \kappa_2 \kappa_3}(B \rightarrow B') \frac{p_A^{\nu_1} p_A^{\nu_2} p_A^{\nu_3}}{s}, \quad (\text{A.8})$$

and the effective production vertex as

$$\Phi_{J/\psi}^{\lambda_2 \kappa_1 \kappa_2}(\mathbf{l}_2, \mathbf{k}_1, \mathbf{k}_2) = \int d\beta_{k_1} \mathcal{S}_{\mu'_2 \nu'_1 \nu'_2}^{\lambda_2 \kappa_1 \kappa_2}(J/\psi) \frac{p_A^{\mu'_2} p_B^{\nu'_1} p_B^{\nu'_2}}{s}. \quad (\text{A.9})$$

It is obvious that an analogous reasoning can be applied to the sum of diagrams describing fusion of the photon with the pomeron in Fig. 3a. The analog of Eq. (A.6) then reads

$$\begin{aligned} \mathcal{M}_{\gamma P} = & -\frac{s}{2!} \frac{4}{(2\pi)^4} \frac{\Phi_P^\gamma(\mathbf{l})}{\mathbf{l}^2} \int \frac{d^2 \mathbf{k}_1}{\mathbf{k}_1^2} \frac{d^2 \mathbf{k}_2}{\mathbf{k}_2^2} \delta^2(\mathbf{k}_1 + \mathbf{k}_2 - \mathbf{k}) \\ & \int d\alpha_{k_1} \mathcal{S}_{\nu_1 \nu_2}^{\kappa_1 \kappa_2}(B \rightarrow B') \frac{p_A^{\nu_1} p_A^{\nu_2}}{s} \int d\beta_{k_1} \mathcal{S}_{\nu'_1 \nu'_2}^{\kappa_1 \kappa_2}(J/\psi) \frac{p_B^{\nu'_1} p_B^{\nu'_2}}{s}, \end{aligned} \quad (\text{A.10})$$

where we introduced the photon coupling to the proton  $\Phi_P^\gamma(\mathbf{l})$  normalized to the proton charge,  $\Phi_P^\gamma(0) = -ie$ . Eq. (A.10) coincides with the impact-factor representation Eq. (18) if the pomeron-photon effective vertex reads

$$\tilde{\Phi}_{J/\psi}^{\kappa_1 \kappa_2}(\mathbf{l}, \mathbf{k}_1, \mathbf{k}_2) = \int d\beta_{k_1} \mathcal{S}_{\mu' \nu'_1 \nu'_2}^{\kappa_1 \kappa_2}(J/\psi) \frac{p_A^{\mu'} p_B^{\nu'_1} p_B^{\nu'_2}}{s} \quad (\text{A.11})$$

and if the definition of the impact-factor for pomeron exchange (A.7) is used for the transition  $h(p_B) \rightarrow h(p_{B'})$ .

## A.2 Derivation of the quark impact-factors (6) and (7)

The quark impact-factor with exchange of the pomeron is defined by Eq. (A.7) specified for a quark target. The  $S$ -matrix corresponding to this transition is described by two diagrams and their colour singlet contribution reads

$$\begin{aligned} & \int d\beta_{l_1} \mathcal{S}_{\mu_1 \mu_2}^{\lambda_1 \lambda_2}(A \rightarrow A') \frac{p_B^{\mu_1} p_B^{\mu_2}}{s} = \\ & -i\bar{g}^2 \frac{\delta^{\lambda_1 \lambda_2}}{2N_c} \int d\beta_{l_1} \left( \frac{1}{\beta_{l_1} + i\epsilon} + \frac{1}{-\beta_{l_1} - \frac{\mathbf{l}^2}{s(1-x_A)} + i\epsilon} \right) = -2\pi \bar{g}^2 \frac{\delta^{\lambda_1 \lambda_2}}{2N_c}, \end{aligned} \quad (\text{A.12})$$

which reproduces Eq. (6).

Similarly, the quark impact factor with exchange of the odderon is defined by Eq. (A.8) specified for a quark target. The  $S$ -matrix corresponding to this transition is described by six diagrams and their colour singlet contribution reads

$$\begin{aligned} & \int d\alpha_{k_3} d\alpha_{k_1} \mathcal{S}_{\nu_1 \nu_2 \nu_3}^{\kappa_1 \kappa_2 \kappa_3}(B \rightarrow B') \frac{p_A^{\nu_1} p_A^{\nu_2} p_A^{\nu_3}}{s} = \\ & -i\bar{g}^3 \frac{d^{\kappa_1 \kappa_2 \kappa_3}}{4N_c} \int d\alpha_{k_3} d\alpha_{k_1} \left( \frac{1}{(\alpha_{k_1} + i\epsilon)(\alpha_{k_1} + \alpha_{k_2} + i\epsilon)} + \frac{1}{(\alpha_{k_1} + i\epsilon)(\alpha_{k_1} + \alpha_{k_3} + i\epsilon)} \right. \\ & + \frac{1}{(\alpha_{k_2} + i\epsilon)(\alpha_{k_2} + \alpha_{k_1} + i\epsilon)} + \frac{1}{(\alpha_{k_2} + i\epsilon)(\alpha_{k_2} + \alpha_{k_3} + i\epsilon)} \\ & \left. + \frac{1}{(\alpha_{k_3} + i\epsilon)(\alpha_{k_3} + \alpha_{k_1} + i\epsilon)} + \frac{1}{(\alpha_{k_3} + i\epsilon)(\alpha_{k_3} + \alpha_{k_2} + i\epsilon)} \right) = i\bar{g}^3 (2\pi)^2 \frac{d^{\kappa_1 \kappa_2 \kappa_3}}{4N_c}, \end{aligned} \quad (\text{A.13})$$

where in the last step we used the fact that  $\alpha_{k_1} + \alpha_{k_2} + \alpha_{k_3} = -\frac{\mathbf{k}^2}{s(1-x_B)}$ . Expression (A.13) reproduces Eq. (7).

## A.3 Derivation of the effective vertices (16) and (21)

The effective vertex (A.9) is given by the contribution of the six diagrams shown in Fig. 5 with the momenta  $l_2 \approx x_A p_A + l_\perp$ ,  $k_j \approx \beta_{k_j} p_B + k_{\perp j}$ ,  $j = 1, 2$ , where  $\beta_{k_1} + \beta_{k_2} \approx x_B$ . Taking into account the definition (14) of the production vertex, the contribution of the

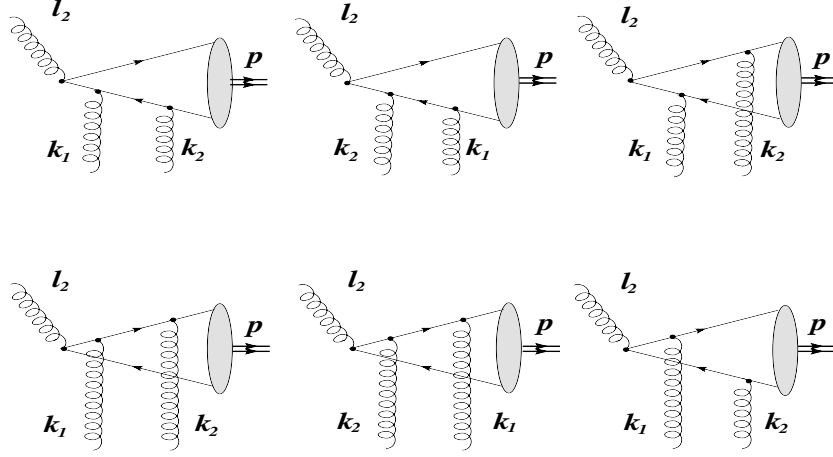


Figure 5: The six diagrams defining the effective vertex  $g + 2g \rightarrow J/\psi$ .

6 diagrams of Fig. 5 is equal to

$$\begin{aligned}
 \int d\beta_{k_1} \mathcal{S}_{\mu'_2 \nu'_1 \nu'_2}^{\lambda_2 \kappa_1 \kappa_2}(J/\psi) \frac{p_A^{\mu'_2} p_B^{\nu'_1} p_B^{\nu'_2}}{s} &= -ig^3 \frac{d^{\lambda_2 \kappa_1 \kappa_2}}{2N_c} \frac{g_{J/\psi}}{s} \int d\beta_{k_1} \\
 \text{Tr} \left\{ \left[ \frac{\hat{p}_A \left( \frac{1}{2} \hat{p}_\perp - \hat{l}_{2\perp} + m_c \right) \hat{p}_B}{4m_c^2 + (\mathbf{p} - \mathbf{l}_2)^2 + \mathbf{l}_2^2} \left( \frac{1}{\beta_{k_1} - x_B - \frac{2\mathbf{k}_2^2 - 2\mathbf{p} \cdot \mathbf{k}_2}{sx_A} + i\epsilon} + \frac{1}{\beta_{k_2} - x_B - \frac{2\mathbf{k}_1^2 - 2\mathbf{p} \cdot \mathbf{k}_1}{sx_A} + i\epsilon} \right) \right. \right. \\
 + \frac{2}{s^2 x_A^2} \hat{p}_B \frac{(\frac{1}{2} \hat{p}_\perp - \hat{k}_{1\perp} + m_c) \hat{p}_A (\hat{k}_{2\perp} - \frac{1}{2} \hat{p}_\perp + m_c) + (\frac{1}{2} \hat{p}_\perp - \hat{k}_{2\perp} + m_c) \hat{p}_A (\hat{k}_{1\perp} - \frac{1}{2} \hat{p}_\perp + m_c)}{(\beta_{k_2} - x_B - \frac{2\mathbf{k}_1^2 - 2\mathbf{p} \cdot \mathbf{k}_1}{sx_A} + i\epsilon)(\beta_{k_1} - x_B - \frac{2\mathbf{k}_2^2 - 2\mathbf{p} \cdot \mathbf{k}_2}{sx_A} + i\epsilon)} \hat{p}_B \\
 \left. \left. - \frac{\hat{p}_B \left( \hat{l}_{2\perp} - \frac{1}{2} \hat{p}_\perp + m_c \right) \hat{p}_A}{4m_c^2 + (\mathbf{p} - \mathbf{l}_2)^2 + \mathbf{l}_2^2} \left( \frac{1}{\beta_{k_1} - x_B - \frac{2\mathbf{k}_2^2 - 2\mathbf{p} \cdot \mathbf{k}_2}{sx_A} + i\epsilon} + \frac{1}{\beta_{k_2} - x_B - \frac{2\mathbf{k}_1^2 - 2\mathbf{p} \cdot \mathbf{k}_1}{sx_A} + i\epsilon} \right) \right] \right. \\
 \left. \hat{\varepsilon}^* \left( \frac{1}{2} \hat{p} + m_c \right) \right\} . \quad (\text{A.14})
 \end{aligned}$$

Calculation of the integral over  $\beta_{k_1}$ , subject to the condition  $\beta_{k_1} + \beta_{k_2} \approx x_B$ , leads to the result

$$\int d\beta_{k_1} \mathcal{S}_{\mu'_2 \nu'_1 \nu'_2}^{\lambda_2 \kappa_1 \kappa_2}(J/\psi) \frac{p_A^{\mu'_2} p_B^{\nu'_1} p_B^{\nu'_2}}{s} = g^3 \frac{d^{\lambda_2 \kappa_1 \kappa_2}}{N_c} V_{J/\psi}(\mathbf{l}_2, \mathbf{k}_1, \mathbf{k}_2) , \quad (\text{A.15})$$

which coincides with Eq. (16). Finally, let us note that the only difference between the pomeron-photon effective vertex (21) and the pomeron-odderon one (16) is the colour factor and the photon coupling. This results in the substitution rule  $gd^{\lambda_2 \kappa_1 \kappa_2} \rightarrow 2eQ_c \delta^{\kappa_1 \kappa_2}$ , from which we recover Eq. (21).

## References

- [1] L. Lukaszuk and B. Nicolescu, Nuovo Cimento Letters **8**, 405 (1973).

- [2] J. Czyżewski, J. Kwieciński, L. Motyka and M. Sadzikowski, Phys. Lett. B **398** (1997) 400 [Erratum-ibid. B **411** (1997) 402].
- [3] R. Engel, D. Y. Ivanov, R. Kirschner and L. Szymanowski, Eur. Phys. J. C **4** (1998) 93.
- [4] L. Motyka and J. Kwieciński, Phys. Rev. D **58** (1998) 117501.
- [5] J. Bartels, M. A. Braun, D. Colferai and G. P. Vacca, Eur. Phys. J. C **20** (2001) 323.
- [6] E. R. Berger, A. Donnachie, H. G. Dosch, W. Kilian, O. Nachtmann and M. Rueter, Eur. Phys. J. C **9** (1999) 491.
- [7] J. Olsson [H1 Collaboration], arXiv:hep-ex/0112012, NEW TRENDS IN HIGH-ENERGY PHYSICS: Experiment, phenomenology, theory: Proceedings. Edited by P.N. Bogolyubov, G.V. Bugrij, L.L. Jenkovszky, 2002.
- [8] C. Ewerz and O. Nachtmann, arXiv:hep-ph/0608082.
- [9] L. Motyka, Phys. Lett. B **637** (2006) 185.
- [10] S. J. Brodsky, J. Rathsman and C. Merino, Phys. Lett. B **461** (1999) 114;  
Ph. Hagler, B. Pire, L. Szymanowski and O. V. Teryaev, Phys. Lett. B **535** (2002) 117 [Erratum-ibid. B **540** (2002) 324]; Eur. Phys. J. C **26** (2002) 261;  
I. F. Ginzburg, I. P. Ivanov and N. N. Nikolaev, Eur. Phys. J. C **32S1** (2003) 23;  
Eur. Phys. J. directC **5** (2003) 02.
- [11] A. Breakstone *et al.*, Phys. Rev. Lett. **54** (1985) 2180.
- [12] C. Ewerz, hep-ph/0306137.
- [13] J. P. Lansberg, Int. J. Mod. Phys. A **21** (2006) 3857.
- [14] A. Schäfer, L. Mankiewicz and O. Nachtmann, Phys. Lett. B **272** (1991) 419.
- [15] I. F. Ginzburg, S. L. Panfil and V. G. Serbo, Nucl. Phys. B **284** (1987) 685; *ibid* Nucl. Phys. B **296** (1988) 569; I. F. Ginzburg and D. Y. Ivanov, Nucl. Phys. B **388** (1992) 376.
- [16] M. Fukugita and J. Kwieciński, Phys. Lett. B **83** (1979) 119; see also J. F. Gunion and D. E. Soper, Phys. Rev. D **15** (1977) 2617 and J. R. Cudell and B. U. Nguyen, Nucl. Phys. B **420** (1994) 669.
- [17] G. A. Schuler, Comput. Phys. Commun. **108** (1998) 279.
- [18] L. N. Lipatov, Sov. J. Nucl. Phys. **23** (1976) 338; E. A. Kuraev, L. N. Lipatov and V. S. Fadin, Sov. Phys. JETP **45** (1977) 199; I. I. Balitsky and L. N. Lipatov, Sov. J. Nucl. Phys. **28** (1978) 822.

- [19] V. A. Khoze, A. D. Martin, M. G. Ryskin and W. J. Stirling, Eur. Phys. J. C **35** (2004) 211.
- [20] H. Navelet, R. Peschanski, C. Royon, L. Schoeffel and S. Wallon, Mod. Phys. Lett. A **12** (1997) 887.
- [21] H1 Collaboration: S. Aid *et al.*, Nucl. Phys. B **472** (1996) 3; H1 Collaboration: C. Adloff *et al.*, Phys. Lett. B **483** (2000) 23; H1 Collaboration: A. Aktas *et al.*, Eur. Phys. J. C **46** (2006) 585.
- [22] ZEUS Collaboration: J. Breitweg *et al.*, Z. Phys. C **75** (1997) 215; Phys. Lett. B **437** (1998) 432; ZEUS Collaboration: S. Chekanov *et al.*, Eur. Phys. J. C **24** (2002) 345.
- [23] J. Bartels, Nucl. Phys. B **175** (1980) 365; J. Kwieciński and M. Praszalowicz, Phys. Lett. B **94** (1980) 413.
- [24] J. Bartels, L. N. Lipatov and G. P. Vacca, Phys. Lett. B **477** (2000) 178.
- [25] R. A. Janik and J. Wosiek, Phys. Rev. Lett. **82** (1999) 709.
- [26] H. G. Dosch, C. Ewerz and V. Schatz, Eur. Phys. J. C **24** (2002) 561.
- [27] V. A. Khoze, A. D. Martin and M. G. Ryskin, Eur. Phys. J. C **18** (2000) 167.
- [28] E. Gotsman, H. Kowalski, E. Levin, U. Maor and A. Prygarin, Eur. Phys. J. C **47** (2006) 655.
- [29] V. A. Khoze, A. D. Martin and M. G. Ryskin, Eur. Phys. J. C **24** (2002) 459.
- [30] S. R. Klein and J. Nystrand, Phys. Rev. Lett. **92** (2004) 1420031.
- [31] M. G. Albrow *et al.*, “FP420: An R&D proposal to investigate the feasibility of installing proton tagging detectors in the 420 m region at LHC”, CERN-LHCC-2005-025.